Inorganic Chemistry
Article

Inorg. Chem. **2011**, *50*, 1991–2001 **1991**
DOI: 10.1021/ic102494k

Novel Pyridazine Based Scorpionate Ligands in Cobalt and Nickel Boratrane Compounds

Gernot Nuss,[†] Gerald Saischek,[†] Bastian N. Harum,[†] Manuel Volpe,[†] Karl Gatterer,[‡] Ferdinand Belaj,[†] and Nadia C. Mösch-Zanetti*,[†]

[†]*Institut für Chemie, Karl-Franzens-Universität Graz, Schubertstrasse 1, A-8010 Graz, Austria, and* [‡]*Institut für Physikalische und Theoretische Chemie, Technische Universität Graz, Stremayrgasse 9, A-8010 Graz, Austria*

Received December 13, 2010

Heating of 6-methylpyridazine-3-thione (HPn^{Me}) and 6-*tert*-butylpyridazine-3-thione (HPn^{tBu}) with potassium borohydride in diphenylmethane in a 3:1 ratio gave two new scorpionate ligands $K[HB(Pn^{Me})_3]$ and $K[HB(Pn^{tBu})_3]$. Single crystal X-ray diffraction analysis of the methyl derivative $K[HB(Pn^{Me})_3]$ revealed a dimeric species with one potassium atom coordinated by six sulfur atoms of two scorpionate ligands and a second potassium atom coordinated by three nitrogen atoms of one of the two ligands as well as by three water molecules. The reaction of $K[HB(Pn^{tBu})_3]$ with nickel(II) chloride or cobalt(II) chloride in CH_2Cl_2 led to the new boratrane compounds $[M\{B(Pn^{tBu})_3\}Cl]$ (M = Ni **1**, Co **3**) where a formal reduction of the metal ions to Ni(I) and Co(I), respectively, and activation of the B−H bond occurred. Similar reactivity was observed by employing $K[HB(Pn^R)_3]$ (R = Me, tBu) and nickel(II) chloride in water. Reaction with cobalt(II) chloride in water also gave boratrane compounds $[Co\{B(Pn^R)_3\}(Pn^R)]$ (R = tBu **4**, Ph **5**), but instead of a chloride a bidentate pyridazinethionate ligand from a defragmentated scorpionate is found in the molecules. The molecular structures of all nickel and cobalt compounds were determined by single crystal X-ray diffraction analyses confirming the formation of boratranes in compounds **1**−**5**. Magnetic measurements confirm the reduced oxidation states and the paramagnetic character of the Ni(I) and Co(I) complexes. Supportive DFT studies were carried out for a better understanding of the electronic nature of the metal−boron bond of the boratrane complexes.

Introduction

Scorpionate ligands have found wide application in coordination chemistry, bioinorganic chemistry[1] and catalysis[2] since the discovery of tris(pyrazolyl)borate (Tp, Figure 1) by Trofimenko in 1966.[3] The versatility of these ligands derives from the numerous possibilities of variation concerning nature, number and position of the substituents in the pyrazole ring which have large electronic and steric effects on the complex. For many years ligand design was limited to pyrazole variations.

In 1996 Reglinski and co-workers introduced a soft analogue of Tp by substituting pyrazolyl by mercaptoimidazolyl rings, tris(mercaptoimidazolyl)borate (Tm), where the three thione sulfur atoms coordinate in a tripodal fashion.[4] This sparked the imagination of researchers so that other mercapto heterocycles were introduced at boron such as tris(thioxotriazolinyl)borate (Tt)[5] and the recently reported tris(mercaptopyridinyl)borate (Tmp).[6] They all show significant differences compared to Trofimenko's original scorpionate. Not only does the softer nature of the coordinating atom (S vs N) lead to a dramatic change of electronic influences but also coordinational flexibility is increased. In the mercapto systems the boron atom and the coordinating atom are connected by a two atom link (N−C) forming eight-membered chelate rings in comparison to a one atom link (N) with six-membered chelates in Tp. The larger chelates lead to a propeller-like arrangement of the three heterocycles in the tripodal ligand upon coordination. Furthermore and most

*Corresponding author. E-mail: nadia.moesch@uni-graz.at.

(1) (a) Tesmer, M.; Shu, M.; Vahrenkamp, H. *Inorg. Chem.* **2001**, *40*, 4022–4029. (b) Kitajima, N.; Fukui, H.; Morooka, Y. *Chem. Commun.* **1988**, 485–486. (c) Holmes, S.; Carrano, C. J. *Inorg. Chem.* **1991**, *30*, 1231–1235. (d) Cleland, W. E., Jr.; Barnhart, K. M.; Yamanouchi, K.; Collison, D.; Mabbs, F. E.; Ortega, R. B.; Enemark, J. H. *Inorg. Chem.* **1987**, *26*, 1017–1025.

(2) (a) Misumi, Y.; Seino, H.; Mizobe, Y. *J. Am. Chem. Soc.* **2009**, *131*, 14636–14637. (b) Blosch, L. L.; Abboud, K.; Boncella, J. M. *J. Am. Chem. Soc.* **1991**, *113*, 7066–7068. (c) Vicente, C.; Shul'pin, G. B.; Moreno, B.; Sabo-Etienne, S.; Chaudret, B. *J. Mol. Catal. A: Chem.* **1995**, *98*, L5–L8. (d) Sanford, M. S.; Henling, L. M.; Grubbs, R. H. *Organometallics* **1998**, *17*, 5384–5389.

(3) (a) Trofimenko, S. *J. Am. Chem. Soc.* **1966**, *88*, 1842–1844. (b) Trofimenko, S. *Scorpionates: The Coordination Chemistry of Polypyrazolylborate Ligands*; Imperial College Press: London, 1999. (c) Pettinari, C. *Scorpionates II: Chelating Borate Ligands*; Imperial College Press: London, 2008.

(4) Garner, M.; Reglinski, J.; Cassidy, I.; Spicer, M. D.; Kennedy, A. R. *Chem. Commun.* **1996**, 1975–1976.

(5) Bailey, P. J.; Lanfranchi, M.; Marchio, L.; Parsons, S. *Inorg. Chem.* **2001**, *40*, 5030–5035.

(6) Dyson, G.; Hamilton, A.; Mitchell, B.; Owen, G. R. *Dalton Trans.* **2009**, 6120–6126.

Published on Web 01/20/2011

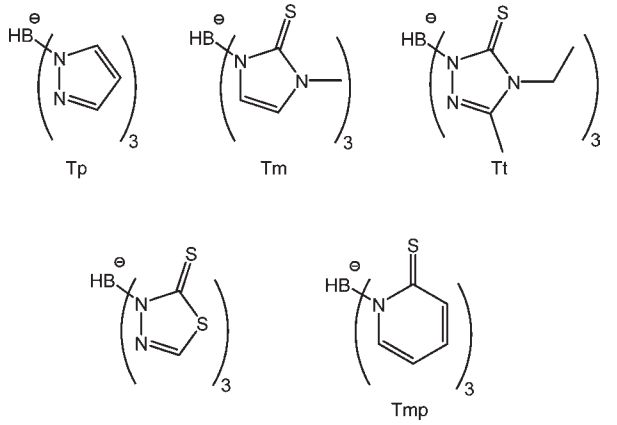

Figure 1. Variation in tripodal scorpionate ligands.

interestingly, activation of the boron bridgehead and formation of metal−borane (metallaboratrane) complexes can be observed. In such compounds a dative M→B bond is believed to occur. They were controversially discussed[7] until in 1999 Hill and co-workers reported the first structural evidence for a metallaboratrane, $[Ru\{B(mim^{Me})_3Ru(CO)(PPh_3)]$ (mim^{Me} = 2-mercapto-1-methylimidazolyl).[8] This complex was synthesized via treatment of the precursor $[Ru(CH{=}CHCPh_2OH)Cl(CO)(PPh_3)_2]$ with $Na[HB(mim^{Me})_3]$ in dichloromethane at room temperature, exhibiting B−H activation of the borate ligand and the formation of a σ dative metal→ boron bond. Boron acts as the Lewis acid (vacant p-orbital) and accepts electrons from a suitable orbital of the metal fragment.[9]

Since the first discovery several metallaboratranes with sulfur containing scorpionate ligands were prepared with various metals.[10] They gained interest because of the ability to act as a "hydride store", where the hydrogen atom can reversibly bind to boron or to the metal, rendering them potential candidates for catalytic applications.[11]

With the two first row transition metals cobalt and nickel only a limited number of examples are known. Rabinovich reported the cobalt complex $[Co\{B(mim^{tBu})_3\}(PPh_3)]BPh_4$,[10f] Tatsumi the nickel complex $[Ni\{B(mim^{tBu})_3\}Cl]$,[10g] and Parkin derivatives of the latter $[Ni\{B(mim^{tBu})_3\}X]$ (X = N_3, NCS or OAc). Furthermore, a nickel boratrane compound is formed with a related triphosphine borane ligand $[Ni\{B(C_6H_4P(iPr)_2)_3\}]$.

Recently, we started to explore the coordination chemistry of pyridazine ligands.[12] The six-membered ring with two adjacent nitrogen atoms belongs to the electron-deficient heterocycles (pK_a values 2.24 for parent pyridazine vs 5.25 for pyridine).[13] Pyridazines without adjacent coordination sites act mostly as monodentate ligands albeit with decreased donor abilities in comparison to pyridine. Thus, in coordination compounds it is mainly found to be involved in macrocyclic ligand systems with two donating substituents adjacent to the two nitrogen atoms.[14] Pyridazines with only one additional donor next to a ring-nitrogen atom leading to bi- or tridentate ligands have been significantly less investigated. We found a convenient synthetic entry into pyridazine ligands that contain one donating substituent in 3-position whereas substituents in 6-position are noncoordinating and can be synthetically fine-tuned leading to a new ligand system with interesting electronic properties.[12]

Our interest in the coordination behavior of the pyridazine heterocycle led us explore its viability as part of scorpionate ligands. Pyridazinones can easily be converted into their sulfur analogues,[15] so that we envisioned the synthesis of an analogue to $K[HB(mim^{Me})_3]$. The six-membered ring, the electron deficient nature and the additional nitrogen being a potential additional donor are likely leading to a diverse ligand system. Variation of the coordinating atom in $[Fe\{HB(mtda^R)_3\}_2]$ ($mtda^R$ = mercaptothiadiazolyl, R = H, Me) has previously shown that the coordination mode can alter the spin state from low spin FeN_6 to high spin paramagnetic FeS_6, respectively.[16] Scorpionate ligands with six-membered heterocycles are rare. Only very recently, Owen and coworkers reported a pyridine-2-thionate containing scorpionate ligand (K[Tmp]) and complexes thereof.[6] The molecular structure of K[Tmp] was found to be polymeric with the potassium atom coordinated by two sulfur atoms of mercaptopyridine and 3-center-2-electron B−H···K interaction. The ligands K[Tmp] and $Na[H_2B(mp)_2]$ (mp = 2-mercaptopyridine) coordinate to copper(I) showing a κ^3-*S*,*S*,*S* and κ^3-*H*,*S*,*S* coordination mode, respectively.

Here, we report the synthesis of novel flexible tris(mercaptopyridazinyl)borate ligands and their coordinational behavior toward nickel(II) and cobalt(II) centers. We found exclusive formation of boratrane compounds as indicated by X-ray diffraction analyses, magnetic measurements and theoretical calculations.

Results and Discussion

Preparation of the Scorpionate Ligands. The pyridazinethiones 6-methylpyridazine-3-thione and 6-phenylpyridazine-3-thione employed in this study were prepared from known pyridazin-3-ones by reaction with phosphorpentasulfide in hot pyridine in good yields according to literature methods.[15] The *tert*-butyl derivative, 6-*tert*-butylpyridazine-3-thione, was synthesized analogously.

(7) (a) Braunschweig, H. *Angew. Chem., Int. Ed.* **1998**, *37*, 1786–1801. (b) Shriver, D. F. *J. Am. Chem. Soc.* **1963**, *85*, 3509–3510. (c) Braunschweig, H.; Wagner, T. *Z. Naturforsch., B: Chem. Sci.* **1996**, *51*, 1618–1620. (d) Braunschweig, H.; Wagner, T. *Chem. Ber.* **1994**, *127*, 1613–1614. (e) Braunschweig, H.; Kollann, C. *Z. Naturforsch., B: Chem. Sci.* **1999**, *54*, 839–842.

(8) Hill, A. F.; Owen, G. R.; White, A. J. P.; Williams, D. J. *Angew. Chem., Int. Ed.* **1999**, *38*, 2759–2761.

(9) (a) Kuzu, I.; Krummenacher, I.; Meyer, J.; Armbruster, F.; Breher, F. *Dalton Trans.* **2008**, 5836–5865. (b) Braunschweig, H.; Kollann, C.; Rais, D. *Angew. Chem., Int. Ed.* **2006**, *45*, 5254–5274.

(10) (a) Crossley, I. R.; Foreman, M. R. S. J.; Hill, A. F.; White, A. J. P.; Williams, D. J. *Chem. Commun.* **2005**, 221–223. (b) Crossley, I. R.; Hill, A. F. *Organometallics* **2004**, *23*, 5656–5658. (c) Crossley, I. R.; Hill, A. F.; Willis, A. C. *Organometallics* **2005**, *24*, 1062–1064. (d) Figueroa, J. S.; Melnick, J. G.; Parkin, G. *Inorg. Chem.* **2006**, *45*, 7056–7058. (e) Foreman, M. R. S. J.; Hill, A. F.; White, A. J. P.; Williams, D. J. *Organometallics* **2004**, *23*, 913–916. (f) Mihalcik, D. J.; White, J. L.; Tanski, J. M.; Zakharov, L. N.; Yap, G. P. A.; Incarvito, C. D.; Rheingold, A. L.; Rabinovich, D. *Dalton Trans.* **2004**, 1626–1634. (g) Senda, S.; Ohki, Y.; Hirayama, T.; Toda, D.; Chen, J.-L.; Matsumoto, T.; Kawaguchi, H.; Tatsumi, K. *Inorg. Chem.* **2006**, *45*, 9914–9925. (h) Pang, K.; Tanski, J. M.; Parkin, G. *Chem. Commun.* **2008**, 1008–1010. (i) Sircoglou, M.; Bontemps, S.; Bouhadir, G.; Saffon, N.; Miqueu, K.; Gu, W.; Mercy, M.; Chen, C.-H.; Foxman, B. M.; Maron, L.; Ozerov, O. V.; Bourissou, D. *J. Am. Chem. Soc.* **2008**, *130*, 16729–16738.

(11) (a) Crossley, I. R.; Hill, A. F. *Dalton Trans.* **2008**, 201–203. (b) Rudolf, G. C.; Hamilton, A.; Orpen, A. G.; Owen, G. R. *Chem. Commun.* **2009**, 553–555.

(12) Grünwald, K. R.; Saischek, G.; Volpe, M.; Belaj, F.; Mösch-Zanetti, N. C. *Eur. J. Inorg. Chem.* **2010**, 2297–2305.

(13) Lide, D. R. *CRC Handbook of Chemistry and Physics*, 88th ed.; Taylor & Francis: 2007.

(14) (a) Weitzer, M.; Brooker, S. *Dalton Trans.* **2005**, 2448–2454. (b) Brooker, S. *Eur. J. Inorg. Chem.* **2002**, 2535–2547.

(15) Arakawa, K.; Miyasaka, T.; Satoh, K. *Chem. Pharm. Bull.* **1977**, *25*, 299–306.

(16) Silva, R. M.; Gwengo, C.; Lindeman, S. V.; Smith, M. D.; Long, G. J.; Grandjean, F.; Gardinier, J. R. *Inorg. Chem.* **2008**, *47*, 7233–7242.

Scheme 1. Preparation of Pyridazine-3-thionyl Based Scorpionate Ligands

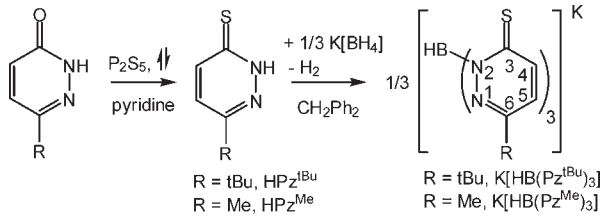

The synthetic method for the preparation of the scorpionate ligands follows those of other scorpionate ligands.[3a,6,8] However, due to the high melting point and the higher tendency of pyridazinethiones to decompose, the method was modified (Scheme 1). Thus, the respective pyridazinethione derivatives were suspended together with potassium borohydride in the ratio 3:1 in diphenylmethane under careful monitoring of the temperature and hydrogen evolution, which was beginning to be evident between 150 and 170 °C. As soon as hydrogen evolution ceased, the increase of the temperature was stopped and the mixture was stirred for an additional 30 to 60 min during which the products started to precipitate. Reaction progress was followed by thin layer chromatography (silica/acetylacetate) where the end of the reaction was indicated by the absence of pyridazinethione. The scorpionate ligands precipitated from the reaction mixture upon cooling and were isolated as yellow solids after workup. Following this procedure we were able to obtain $K[HB(Pn^{Me})_3]$ and $K[HB(Pn^{tBu})_3]$ in analytically pure form as described in the Experimental Section. The phenyl substituted ligand $K[HB(Pn^{Ph})_3]$ gave an impure material evidenced by ^{13}C NMR spectroscopy and elemental analysis independent of the ratio of $[BH_4]^-$ vs pyridazinethione employed. Any attempts to purify the ligand were unsuccessful due to similar solubility properties. With the methyl or *tert*-butyl substituted ligands lower ratios than 3:1 yielded exclusively the trisubstituted $K[HB(Pn^R)_3]$ (R = Me, tBu) compounds.

The potassium salts are soluble in polar organic solvents as well as in water; however, they are completely insoluble in less polar solvents such as diethyl ether or cyclohexane. They are stable in aqueous solutions or dissolved in DMSO as NMR samples remain unchanged for 24 h. NMR spectroscopy of the salts in deuterated dimethyl sulfoxide (DMSO-d_6) confirmed the formation of the scorpionate ligands indicated by significant shifts of all resonances in the ^1H NMR and ^{13}C NMR spectra in comparison to the pyridazinethione derivatives. For example, the resonance of the protons of the three equivalent *tert*-butyl groups in the ^1H NMR spectrum of $K[HB(Pn^{tBu})_3]$ appears at 0.91 ppm, which corresponds to a high field shift of 0.29 ppm vs those of HPn^{tBu}. The two protons of the pyradizine ring appear as two characteristic doublets in the aromatic region in the potassium salts where as in HPn^R one of the two is additionally coupled to the NH proton (dd).

Stretching vibrations of the B−H in the infrared spectra are usually found around 2400 cm^{-1} and are significantly shifted when the hydrogen is coordinated to a metal.[17] Surprisingly, infrared spectroscopy of all potassium salts did not show a B−H stretching vibration, which would have been a possible tool to distinguish between a trisubstituted and a tetrasubstituted product in the phenyl derivative.

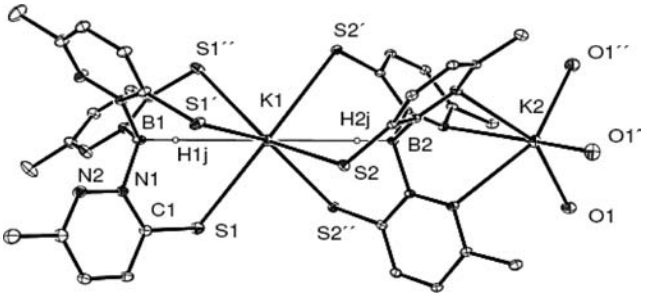

Figure 2. Molecular view of $[K_2\{HB(Pn^{Me})_3\}_2(H_2O)_3]$. Hydrogen atoms have been omitted for clarity except the two H atoms at boron.

Table 1. Selected Bond Lengths (Å) and Angles (deg) of $[K_2\{HB(Pn^{Me})_3\}_2(H_2O)_3]$

K1−S1	3.2689(18)	K1···B1	3.531
K1−S2	3.3067(16)	K1···B2	3.502
K2−N4	3.001(4)	S1−K1−S1′[a]	88.82(5)
K1−H1J	2.529(2)	S1′−K1−S2	75.95(3)
K1−H2J	2.500(2)	S1−K1−S2	114.77(3)
B1−H1J	1.002(9)	N1′−B1-N1	111.6(4)
K2−O1	2.644(4)	N3′−B2-N3	110.5(3)

[a] (′) $-y + 1, x - y, z$.

Single crystals of the methyl derivative $K[HB(Pn^{Me})_3]$ suitable for X-ray diffraction analysis were obtained from a methanol solution by slow evaporation of the solvent. A molecular view is shown in Figure 2, and selected bond lengths and angles are given in Table 1. Crystallographic parameters are given in Table 6. The molecular structure analysis of $K[HB(Pn^{Me})_3]$ revealed an interesting dimeric compound consisting of two anionic scorpionate ligands $[HB(Pn^{Me})_3]^-$, two K^+ ions and three coordinated water molecules. Both ligands coordinate to one of the two potassium ions in κ^4-*H*,*S*,*S*,*S* fashion leading to an octacoordinate metal atom. The other potassium atom is coordinated be the three nitrogen atoms of one of the two scorpionate ligands in κ^3-*N*,*N*,*N* fashion. The remaining three coordination sites of K^+ are saturated by three water molecules leading to an octahedral surrounding. A 3-fold axis runs through the two potassium atoms of the dimeric molecule rendering all potassium sulfur bonds to one ligand identical (K1−S1 3.268(2) Å and K1−S2 3.307(2) Å). The hydrogen atom at boron was inserted at a calculated position while the hydrogen atoms on water were not located. The distances between boron and potassium (K1···B1 3.531 Å and K1···B2 3.502 Å) are long enough to accommodate a hydrogen atom. Such a κ^4-*H*,*S*,*S*,*S* coordination has also been found in the lead compound $[Pb\{Tm^{Ph}\}_2]$ employing a mercapto imidazolyl scorpionate.[17a] The structure is remarkable since the pyridazinethione coordinates to a metal center via both the sulfur and the nitrogen atom. Whereas the coordination of the thio functionality is to be expected, that of the nitrogen atom is surprising. Pyridazine belongs to the electron-deficient heterocycles, and thus the tendency to act as a bridging ligand is low.[18] Here, the electrophilic

(17) (a) Bridgewater, B. M.; Parkin, G. *Inorg. Chem. Commun.* **2000**, *3*, 534–536. (b) Silva, R. M.; Gwengo, C.; Lindeman, S. V.; Smith, M. D.; Gardinier, J. R. *Inorg. Chem.* **2006**, *45*, 10998–11007.

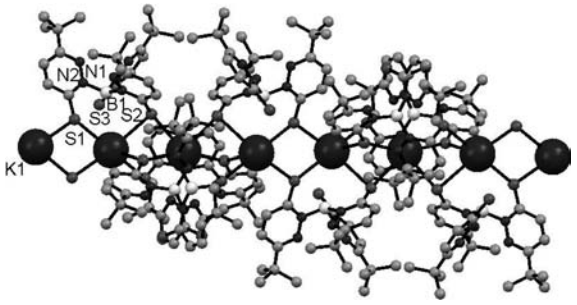

Figure 3. View of the extended structure of $K[HB(Pn^{tBu})_3]$. Hydrogen atoms have been omitted for clarity.

potassium cation allows coordination despite the decreased electron density at nitrogen. This structural situation is in contrast to that of the mercaptothiadiazolyl scorpionate ligand $K[HB(mtda)_3]$ where a polymeric chain is formed with a head to tail arrangement of the scorpionate ligand.[17b] Thus, all potassium atoms are coordinated by three sulfur atoms of one and three nitrogen atoms of a second ligand as well as by an acetonitrile molecule. Similar to $K[HB(Pn^{Me})_3]$, the cations are involved in a 3-center-2-electron B−H···K interaction. A related structure was found in the mercaptothiadiazolyl system by crystallizing a mixed potassium sodium salt of the type $NaK[HB(mtda)_3]_2$ where the softer potassium ions are coordinated by six sulfur atoms of two ligands and the sodium ions by six nitrogen atoms in a polymeric chain.[17] Apparently, in the mtda systems the coordination strength of sulfur and nitrogen toward alkali metals is comparable with a softer side at S whereas in the pyridazinyl system coordination via sulfur is clearly favored over the nitrogen atom of the electronically poor heterocycle.

Single crystals were also obtained of the *tert*-butyl derivative $K[HB(Pn^{tBu})_3]$ from wet chloroform solution confirming its formation and connectivity; however, the quality of the data does not allow discussion of bond lengths and angles. The molecular structure is different from that of the methyl derivative as coordination of the nitrogen atoms is not observed presumably prevented by the larger *tert*-butyl groups. An extended structure is formed in which two crystallographically not equivalent potassium atoms are coordinated by two sulfur atoms and by the hydrogen atom of the B−H bond. The distance between the third sulfur and potassium is significantly longer (K1···S3−4.39 Å), arguing against a bonding interaction. The asymmetric unit is shown in Figure 3. Despite the low quality of the structural data we are fairly convinced of the structural situation as it is similar to the related pyridine derivative recently described by Owen and co-workers.[6]

Preparation of Cobalt and Nickel Complexes. The coordination chemistry of the novel scorpionate ligands toward cobalt and nickel ions was investigated.

The reaction of nickel chloride ($NiCl_2$) with $K[HB(Pn^{tBu})_3]$ in dichloromethane affords an interesting boratrane compound of the type $[Ni\{B(Pn^{tBu})_3\}Cl]$ (**1**) where a B−H bond activation occurred under formal reduction of

(18) Allan, J. R.; Barnes, G. A.; Brown, D. H. *J. Inorg. Nucl. Chem.* **1971**, *33*, 3765–3771.

Scheme 2. Syntheses of the Nickel Boratranes $[Ni\{B(Pn^{tBu})_3\}Cl]$ (**1**) and $[Ni\{B(Pn^{Me})_3\}Cl]$ (**2**)

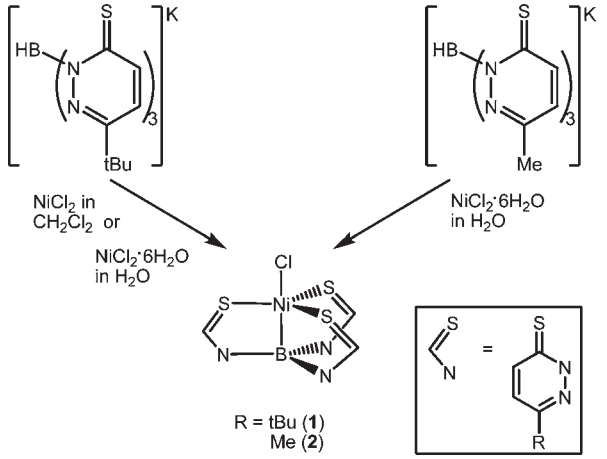

Scheme 3. Syntheses of the Cobalt Boratranes $[Co\{B(Pn^{tBu})_3\}Cl]$ (**3**) and $[Co\{B(Pn^{tBu})_3\}(Pn^{tBu})]$ (**4**)

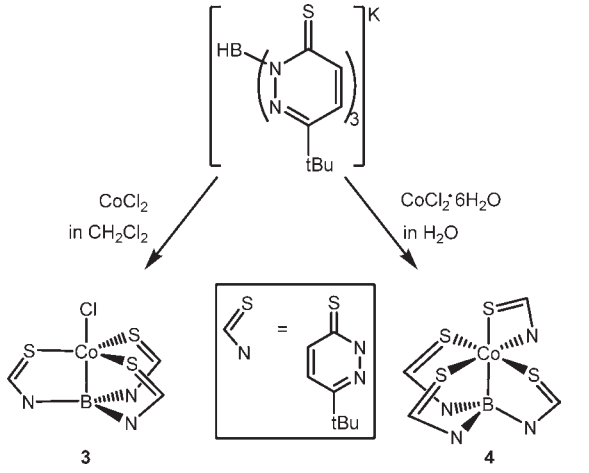

the nickel center to Ni(I) under concurrent formation of a direct Ni−B dative bond (Scheme 2). After workup the red powder was recrystallized from a methanolic solution. The reaction of aqueous nickel chloride ($NiCl_2 \cdot 6H_2O$) with $K[HB(Pn^{tBu})_3]$ in water gave the same compound after workup and crystallization evidenced by X-ray crystallography. Similarly, the reaction of the methyl substituted scorpionate ligand $K[HB(Pn^{Me})_3]$ with $NiCl_2 \cdot 6H_2O$ in water gave the boratrane complex $[Ni\{B(Pn^{Me})_3\}Cl]$ (**2**). The compounds precipitate from the water solution and appropriate workup leads to red crystalline solids. The paramagnetic boratrane compounds $[Ni\{B(Pn^{R})_3\}Cl]$ (R = tBu, Me) are stable in air, soluble in acetone, chloroform, dichloromethane or dimethyl sulfoxide, but insoluble in diethyl ether, toluene or water. Electrospray ionization mass spectrometry (ESI-MS) shows the $[Ni\{B(Pn^{R})_3\}]^+$ fragment, consistent with a fragmentation under loss of the chloride ligand. Despite the impure nature of the phenyl derivative of the scorpionate ligand, synthesis of $[Ni\{B(Pn^{Ph})_3\}Cl]$ was attempted. Similar to **1** and **2** a red powder was obtained after workup. Mass spectrometry of this material shows a corresponding peak for $[Ni\{B(Pn^{Ph})_3\}]^+$ with the correct isotopic pattern (m/z 630 ($[M - Cl]^+$) pointing to its

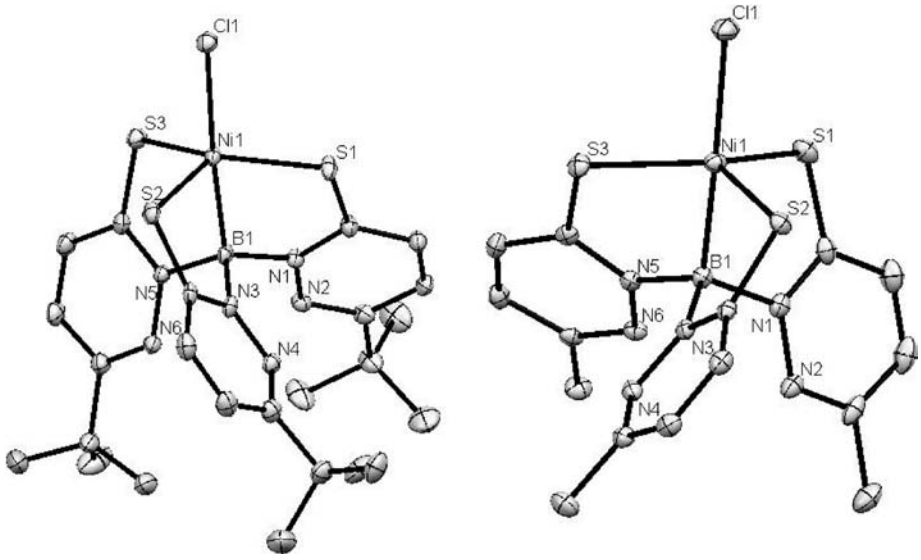

Figure 4. Molecular view of [Ni{B(Pn^{tBu})$_3$}Cl] (**1**) and [Ni{B(Pn^{Me})$_3$}Cl] (**2**). Compound **2** crystallizes with a molecule of (SPn^{Me})$_2$ which is not shown.

formation, but we were unable to purify it as no crystals could be obtained.

The reaction of cobalt chloride ($CoCl_2$) and K[HB(Pn^{tBu})$_3$] in dichloromethane showed formation of a similar boratrane compound [Co{B(Pn^{tBu})$_3$}Cl] (**3**) (Scheme 3) again under formation of a dative Co−B bond and formal reduction of the metal center from Co(II) to Co(I). After appropriate workup of the reaction the dark green suspension was recrystallized from dichloromethane, giving dark green crystals. The paramagnetic boratrane compound is stable in air, soluble in acetone, chloroform, dichloromethane or dimethyl sulfoxide, but insoluble in diethyl ether, toluene or water. When applying electrospray ionization mass spectrometry (ESI-MS), a [Co{B(Pn^{tBu})$_3$}]$^+$ fragment can be found which shows the defragmentation of the complex under loss of the chloride ligand.

Surprisingly, the reaction employing aqueous cobalt chloride ($CoCl_2 \cdot 6H_2O$) and K[HB(Pn^{tBu})$_3$] in water affords a different paramagnetic boratrane complex of the type [Co{B(Pn^{tBu})$_3$}(Pn^{tBu})] (**4**) as shown in Scheme 3. In contrast to **3**, the cobalt atom is additionally coordinated by a bidentate pyridazinethionyl ligand (Pn^{tBu})$^-$ which presumably was formed due to degradation of the scorpionate ligand. The compound precipitates from water, and appropriate workup leads to a dark green, almost black crystalline solid. Its solubility is similar to that of **3**. ESI-MS shows the [Co{B(Pn^{tBu})$_3$}]$^+$ fragment consistent with a fragmentation under loss of the (Pn^{tBu})$^-$ ligand. The methyl derivative [Co{B(Pn^{Me})$_3$}(Pn^{Me})] is again presumably also accessible according to ESI-MS (m/z 445 ([M − Pn^{Me}]$^+$); however, we were as yet not able to obtain it in crystalline form. In the analogous reaction employing the phenyl derivative of the pyridazinyl based scorpionate ligand in water we were able to obtain few crystals suitable for X-ray diffraction analysis also revealing the formation of the analogous boratrane compound [Co{B(Pn^{Ph})$_3$}(Pn^{Ph})] (**5**). Although the small amount of isolated crystals prevented further characterization, we believe the report of the molecular structure of **5** is important as it gives evidence for a general reactivity of these type of ligands with aqueous cobalt chloride.

The mechanism of formation for the here presented boratrane complexes is as yet unclear. All ESI-MS spectra of the crude materials obtained after workup reveal a peak for the disulfide of the respective pyridazinethiones [(^{R}PnS−SPn^R) + H]$^+$ (R = tBu m/z 335; R = Me m/z 251; R = Ph m/z 375). This is consistent with the X-ray structure analysis of [Ni{B(Pn^{Me})$_3$}Cl] which revealed next to the nickel complex one molecule of ^{Me}PnS−SPn^{Me} in the asymmetric unit (vide infra). The disulfide represents an oxidized derivative of the deprotonated pyridazinethione. Thus, it seems likely that the divalent metal acts as the oxidizing agent for the ligand thereby being reduced from Ni(II) to Ni(I), and Co(II) to Co(I), respectively. Subsequently, the oxidizing environment leads to the formation of the disulfide. This would explain the relatively low isolated yields. It is worth noting that mass spectrometry gave no evidence of formation of homoleptic compounds of the type [M{HB(Pn^R)$_3$}$_2$], that are easily formed with imidazolyl based scorpionate ligands.[17a,19]

Molecular Structures of the Boratrane Compounds. X-ray diffractions analyses were determined of compounds [Ni{B(Pn^R)$_3$}Cl] (R = tBu **1**, Me **2**), [Co{B(Pn^{tBu})$_3$}Cl] (**3**), and [Co{B(Pn^R)$_3$}(Pn^R)] (R = tBu **4**, Ph **5**). Molecular views are depicted in Figures 4, 5 and 6. Selected bond lengths and angles are listed in Tables 2 and 3, and crystallographic data are shown in Table 6.

The geometry at the nickel atom in **1** and **2** is best described as distorted trigonal bipyramidal (τ 0.80 for **1** and 0.78 for **2**) with three sulfur atoms in equatorial positions, a chlorine and a boron atom in axial positions. The B−Ni−Cl angle is almost perfectly linear (177.49(11) in **1** and 177.80(6)° in **2**); however, the three S−Ni−S angles vary significantly and range between 105.35(2) and 131.12(2)°, illustrating the distortion. The nickel boron interaction can be considered as a direct dative bond from the transition metal to boron (2.016(3) Å in **1** and 2.034(2)

(19) (a) Kimblin, C.; Churchill, D. G.; Bridgewater, B. M.; Girard, J. N.; Quarless, D. A.; Parkin, G. *Polyhedron* **2001**, *20*, 1891–1896. (b) Kimblin, C.; Bridgewater, B. M.; Hascall, T.; Parkin, G. *Dalton Trans.* **2000**, 1267–1274. (c) Slavin, P. A.; Reglinski, J.; Spicer, M. D.; Kennedy, A. R. *Dalton Trans.* **2000**, 239–240.

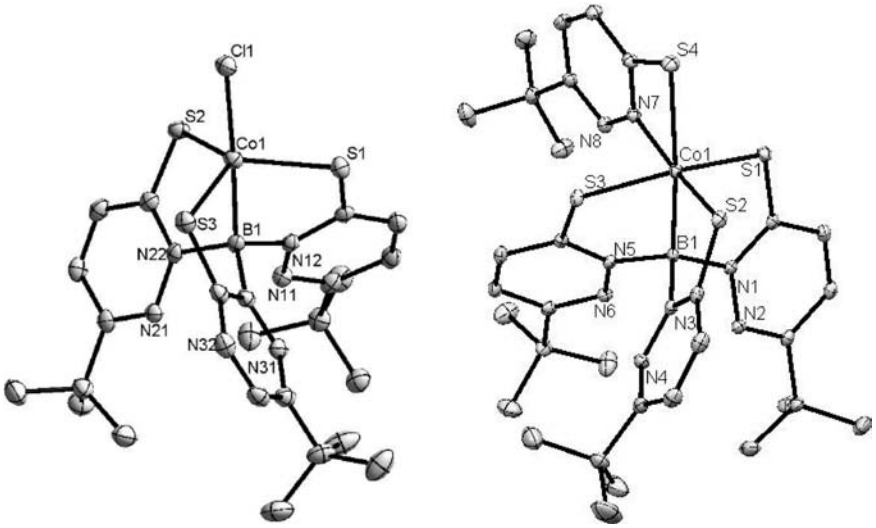

Figure 5. Molecular view of the cobalt complexes [Co{B(Pn^{tBu})$_3$}Cl] (**3**) and [Co{B(Pn^{tBu})$_3$}(Pn^{tBu})] (**4**).

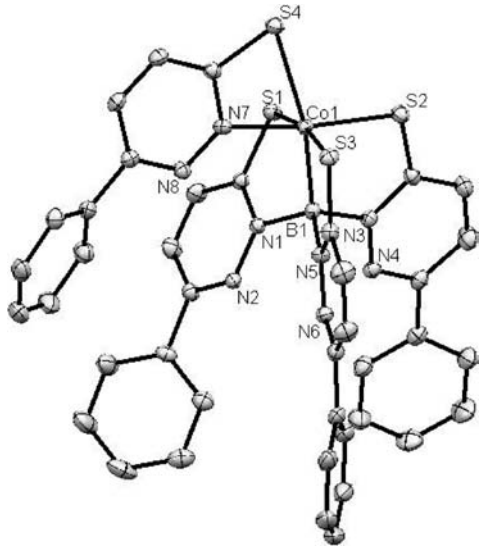

Figure 6. Molecular view of the cobalt complex [Co{B(Pn^{Ph})$_3$}(Pn^{Ph})] (**5**). Selected bond distances (Å) and angles (deg): Co1−B1 1.984(3), Co1−S1 2.2564(6), Co1−S2 2.2236(7), Co1−S4 2.4867(7), Co1−N7 1.927(2), B1−Co1−S4 168.83(8), N7−Co1−S4 69.30(6), S1−Co1−S3 169.59(3), N1−B1−N5 113.76(19).

Å in **2**). These distances are slightly shorter compared to the related boratrane compound with thioimidazolyl substituents ([Ni{B(mim^{tBu})$_3$}Cl] Ni−B 2.108(4) Å).[10g] The shorter bonds lengths found in the here described compounds are likely due to the more electron-deficient heterocycle involved leading to a more electrophilic boron center and thus to a stronger donor bond from the nickel to the boron atom. In contrast, the nickel boron distances in the boryl complex [(PNP)Ni(Bcatechol)] (PNP = N[2-P($CHMe_2$)$_2$-4-methylphenyl]$_2^-$) is with 1.9091(18) Å significantly shorter.[20] Due to the six-membered rings of the pyridazine based ligands the three heterocycles are paddlewheel-like twisted around the metal. This leads to significantly larger sulfur nickel chlorine angles (94.85(2) to 100.080(18)°) in comparison to the imidazolyl based boratrane [Ni{B(mim^{tBu})$_3$}Cl] (91.24(4) to 93.76(4)°).[10g]

Table 2. Selected Bond Lengths (Å) and Angles (deg) of the Nickel Complexes **1** and **2**

	1	**2**
Ni1−B1	2.016(3)	2.034(2)
Ni1−S1	2.2777(10)	2.2381(5)
Ni1−S2	2.2678(10)	2.2658(5)
Ni1−S3	2.2989(10)	2.2757(5)
Ni1−Cl1	2.3171(9)	2.3249(5)
S1−C1	1.723(3)	1.708(2)
S2−C9/C6	1.714(3)	1.7140(18)
S3−C17/C11	1.711(3)	1.7163(18)
B1−N1	1.541(4)	1.550(2)
B1−N3	1.540(4)	1.549(2)
B1−N5	1.539(4)	1.549(2)
S1−Ni1−S2	114.77(3)	105.35(2)
S2−Ni1−S3	111.16(4)	119.237(19)
S1−Ni1−S3	129.27(4)	131.12(2)
B1−Ni1−S1	83.63(10)	85.27(6)
B1−Ni1−S2	83.10(10)	81.99(6)
B1−Ni1−S3	81.54(10)	82.25(6)
S1−Ni1−Cl1	96.56(4)	94.85(2)
S2−Ni1−Cl1	99.07(3)	100.080(18)
S3−Ni1−Cl1	96.45(4)	96.047(19)
B1−Ni1−Cl1	177.49(11)	177.80(6)

The geometry of the cobalt boratrane **3** is similar to the nickel complexes, exhibiting an almost linear B1−Co1−Cl1 angle (177.64(9)). The distorted trigonal bipyramidal geometry is substantiated by the varying S−Co−S angles between 115.13(3) and 118.99(3)° for S1−Co1−S3 and S2−Co1−S3, respectively. The Co−B distance 2.068(3) Å is in the range of compounds **1** and **2**, hence indicating a metal to boron dative bond which is significantly shorter compared to Rabinovich's other cobalt boratrane bearing the thioimidazolyl moiety (2.132(4) Å in [Co{B(mim^{tBu})$_3$}(PPh_3)][BPh_4]).[10f] The Co−Cl bond is slightly shorter compared to compounds **1** and **2** (2.3025(8) vs 2.3171(9) and 2.3249(5), respectively). The three pyridazines are paddlewheel-like twisted around the boron, therefore giving a significantly larger sulfur cobalt chlorine bond (101.36(3)° for S1−Co1−Cl1) compared to the ideal trigonal bipyramidal geometry.

(20) Adhikari, D.; Huffman, J. C.; Mindiola, D. J. *Chem. Commun.* **2007**, 4489–4491.

Table 3. Selected Bond Lengths (Å) and Angles (deg) of the Cobalt Complexes [Co{B(Pn^{tBu})$_3$}Cl] (**3**) and [Co{B(Pn^{tBu})$_3$}(Pn^{tBu})] (**4**)

3		**4**			
Co1−B1	2.068(3)	Co1−B1	2.0041(18)	S2−Co1−S4	99.502(16)
Co1−S1	2.2988(8)	Co1−S1	2.2190(4)	S2−Co1−B1	85.02(5)
Co1−S2	2.2858(8)	Co1−S2	2.2315(5)	S3−Co1−S4	96.296(16)
Co1−S3	2.2855(8)	Co1−S3	2.2746(4)	S3−Co1−B1	80.89(5)
Co1−Cl1	2.3025(8)	Co1−S4	2.4886(5)	S3−Co1−N7	83.21(4)
S1−C13	1.721(3)	Co1−N7	1.9521(14)	B1−Co1−N7	106.22(6)
S2−C23	1.721(3)	S1−C1	1.6910(16)	N7−Co1−S4	69.11(4)
S3−C33	1.709(3)	S2−C9/C11	1.7087(17)	N1−B1−N3	107.78(12)
B1−N12	1.539(4)	S3−C17/C21	1.7154(16)	N1−B1−N5	114.55(13)
B1−N22	1.534(4)	S4−C25/C31	1.7220(17)	N3−B1−N5	104.08(12)
B1−N32	1.549(4)	B1−N1	1.556(2)		
S1−Co1−S2	115.13(3)	B1−N3	1.582(2)		
S2−Co1−S3	118.99(3)	B1−N5	1.553(2)		
S1−Co1−S3	118.51(3)	B1−Co1−S4	174.90(5)		
B1−Co1−S1	81.00(9)	S1−Co1−S3	164.827(18)		
B1−Co1−S2	80.60(9)	N7−Co1−S2	168.08(4)		
B1−Co1−S3	81.09(9)	S1−Co1−S2	94.767(17)		
S1−Co1−Cl1	101.36(3)	S1−Co1−S4	93.571(16)		
S2−Co1−Cl1	98.39(3)	S1−Co1−B1	88.37(5)		
S3−Co1−Cl1	97.62(3)	S1−Co1−N7	89.60(4)		
B1−Co1−Cl1	177.64(9)	S2−Co1−S3	94.939(17)		

X-ray diffraction analyses of the cobalt boratrane compounds **4** and **5** reveal the metal to be coordinated by a [B(Pn^R)$_3$] ligand and a η^2-Pn^R ligand in a distorted octahedral geometry. The sulfur atom of Pn^R is coordinated trans to the boron atom of the [B(Pn^R)$_3$] moiety. The B1−Co1−S4 angles deviate significantly from linearity (174.90(5)° in **4** and 168.83(8) in **5**). Also the small bite angle of the pyridazinethionyl ligand (N7−Co1−S4 69.11(4)° in **4** and 69.30(6)° in **5**) leads to distortion. The S1−Co1−S3 angles are 164.827(18)° in **4** and 169.59(3)° in **5**, which is significantly more linear compared to those in **1**, **2** and **3**. This leads to distortion at boron where the N1−B1−N5 angle is significantly larger than the ideal tetrahedral angle (114.55(13)° in **4** and 113.76(19)° in **5**) pointing to high coordinative flexibility in this type of ligands. This flexibility is also found in related trismercaptoimidazolyborates.[10f] Similar to the trigonal bipyramidal cobalt boratrane and the nickel compounds, the dative B1−Co1 bond lengths are with 2.0041(18) Å in **4** and 1.984(3) Å in **5** shorter than the only other cobaltoboratrane complex described by Rabinovich and co-workers (2.132(4) Å in [Co{B(mim^{tBu})$_3$}(PPh_3)][BPh_4]).[10f]

Magnetic Properties. Measurements of the magnetic susceptibilities of compounds **1**−**4** in the solid state at room temperature were performed with a Faraday balance confirming the paramagnetic nature of the boratranes, which was already indicated by the absence of resonances in the NMR spectra. Each sample was measured at different magnetic fields to exclude the presence of ferromagnetic impurities. All four samples showed no noteworthy field dependency. The reported values for the molar susceptibilities listed in Table 4 refer to the highest field strengths, where the best signal-to-noise ratio is obtained. The measured diamagnetic susceptibility of the pure ligands served as the diamagnetic correction factor. The measured magnetic susceptibilities χ_M allowed the calculation of the number of unpaired electrons.

Comparison of the experimentally determined susceptibilities and the thereof calculated number of unpaired electrons agrees well with the formulation of a d^9 nickel(I) center with one unpaired electron and with a d^8 cobalt(I) center with two unpaired electrons.

Table 4. Molar Magnetic Susceptibilities, Effective Moments and Numbers of Unpaired Electrons for the Ligands and Compounds **1**−**4**

			no. of unpaired electrons	
compound	χ_M [m^3/mol]	μ_{eff}[a]	exptl	theor
K[HB(Pn^{Me})$_3$]	-2.88×10^{-9}			
K[HB(Pn^{tBu})$_3$]	-1.70×10^{-9}			
1	1.99×10^{-8}	1.93	1.18	1
2	1.93×10^{-8}	1.90	1.15	1
3	5.25×10^{-8}	3.14	2.30	2
4	3.95×10^{-8}	2.72	1.90	2

[a] Effective moment.

Theoretical Calculations. For a better understanding of the bonding situation in boratrane complexes theoretical calculations were performed. Density functional theory (DFT) methods are often chosen for studies of transition metal complexes even if they do not always produce accurate spin state energy differences.[21] These energy differences highly depend on the amount of exact exchange of the density functional. Therefore, the two boratrane complexes [Co{B(Pn^H)$_3$}Cl] and [Ni{B(Pn^H)$_3$}Cl] were investigated with three density functionals consisting of different amount of exact exchange, BH-LYP,[22] B3-LYP[22b,c,23] and B-P,[22a,24] respectively. For both complexes, DFT studies with all three functionals agree with the experimentally determined spin. However, the hybrid density functional B3-LYP seems to reproduce the experimental geometries and spin state energetics in the best way and was therefore the functional of choice.

Calculations showed that the energetically favored triplet spin state of [Co{B(Pn^H)$_3$}Cl] features a trigonal bipyramidal structure, whereas reduction of multiplicity

(21) (a) Cramer, C. J.; Truhlar, D. G. *Phys. Chem. Chem. Phys.* **2009**, *11*, 10757–10816. (b) Ghosh, A.; Taylor, P. R. *Curr. Opin. Chem. Biol.* **2003**, *7*, 113–124. (c) Harvey, J. N. *Annu. Rep. Prog. Chem., Sect. C: Phys. Chem.* **2006**, *102*, 203–203.

(22) (a) Becke, A. D. *Phys. Rev. A* **1988**, *38*, 3098–3100. (b) Becke, A. D. *J. Chem. Phys.* **1993**, *98*, 1372–1377. (c) Lee, C.; Yang, W.; Parr, R. G. *Phys. Rev. B* **1988**, *37*, 785–789.

(23) Becke, A. D. *J. Chem. Phys.* **1993**, *98*, 5648–5652.

(24) Perdew, J. P. *Phys. Rev. B* **1986**, *33*, 8822–8824.

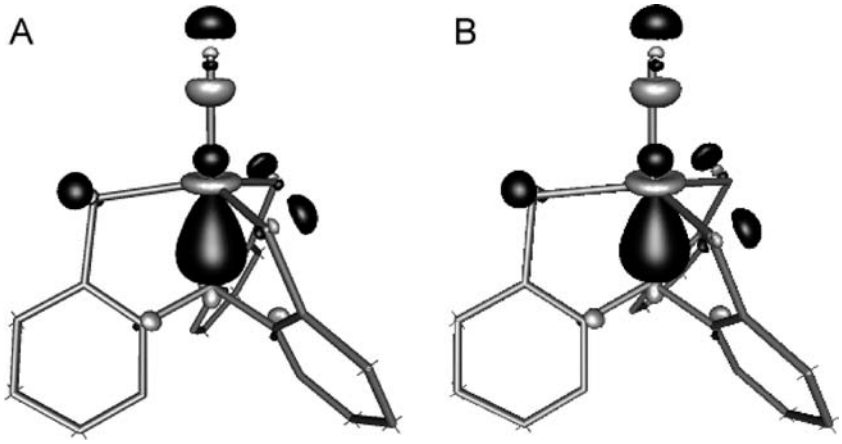

Figure 7. (A) HOMO−3 of complex [Co{B(Pn^H)$_3$}Cl] and (B) HOMO−2 of complex [Ni{B(Pn^H)$_3$}Cl] at the B3-LYP def2-TZVP level of theory.

Table 5. Electronic and Geometric Properties for the Complexes [Co{B(Pn^H)$_3$}Cl] and [Ni{B(Pn^H)$_3$}Cl] at the B3LYP def2-TZVP Level of Theory

					$D(\alpha)-D(\beta)^d$	
	$M_s{}^a$	$E_{rel}{}^b$/kJ/mol	d(M···B)/Å	SEN^c (M···B)	M	B
[Co{B(Pn^H)$_3$}Cl]	1	64	1.97	0.838		
	3	0	2.12	0.646	1.95	−0.10
	5	67	2.85	0.182	2.67	0.37
[Ni{B(Pn^H)$_3$}Cl]	2	0	2.05	0.672	0.92	−0.06
	4	80	2.97	0.150	1.63	0.36

[a] Multiplicity. [b] Spin state energy difference: $E(M_S) - E(3)$ for [Co{B(Pn^H)$_3$}Cl] and $E(M_S) - E(2)$ for [Ni{B(Pn^H)$_3$}Cl]. [c] Shared electron number as calculated by population analysis based on molecular orbitals. [d] Difference in spin density.

to the singlet spin state leads to a square pyramidal geometry with all sulfur atoms and the chlorine atom in one plane. The cobalt−boron bond distance for this low spin state decreases from 2.12 to 1.97 Å, whereas the shared electron number (SEN) increases from 0.646 to 0.838. In contrast, increase of multiplicity to a spin state with four unpaired electrons results in excess α-spin density on both cobalt and boron thus weakening the Co−B bond. This quintet spin state features a slightly distorted tetrahedral geometry with a SEN of 0.182 for the Co−B pair. Consequently, the triplet spin state is in best agreement with the experimental set of data. The SEN of 0.646 for the triplet spin state clearly indicates a polar σ-bond between the cobalt and boron in the dominant triplet state. As shown by molecular orbitals analysis, the HOMO−3 of the triplet state in [Co{B(Pn^H)$_3$}Cl] clearly supports a cobalt−boron σ-bond (as shown in Figure 7). Natural population analysis (NPA) on the three different spin states of complex [Co{B(Pn^H)$_3$}Cl] support these observations. The excess α-spin density of the triplet state is mainly localized on the cobalt atom whereas there is small excess of β-spin density on the boron atom. This is not the case for the quintet state which additionally features a large excess of α-spin density on the boron atom thus weakening the Co−B bond.

Analogous observations were obtained by investigating the doublet and quartet spin states of [Ni{B(Pn^H)$_3$}Cl]. In comparison to the triplet state of [Co{B(Pn^H)$_3$}Cl], the experimentally and computationally determined shorter metal−boron bond distance of the doublet spin state of [Ni{B(Pn^H)$_3$}Cl] together with the increased SEN of 0.672 indicates a slightly stronger σ-bond. In analogy to [Co{B(Pn^H)$_3$}Cl] the excess α-spin density is mainly localized on the metal, whereas there is a small excess of β-spin density on the boron atom. A high spin quartet state of [Ni{B(Pn^H)$_3$}Cl] shows a geometrical and electronical behavior similar to that of the quintet spin state of [Co{B(Pn^H)$_3$}Cl] (Table 5). The cobalt boron bond is broken thus leading to a distorted tetrahedral geometry which is again energetically less favored. Consequently, population analysis supports a polar metal−boron bond for the energetically favored spin states of both complexes, [Co{B(Pn^H)$_3$}Cl] and [Ni{B(Pn^H)$_3$}Cl], respectively.

Conclusions

We have prepared new scorpionate ligands based on pyridazinethione heterocycles of the type K[HB(Pn^R)$_3$] (Pn = pyridazine-3-thione; R = Me, tBu, Ph). The molecular structure of the methyl derivative determined by X-ray diffraction analysis revealed a dimer with one potassium being coordinated by six sulfur atoms of two scorpionate ligands and the second potassium by three nitrogen atoms of one scorpionate and three water molecules. The tripodal ligands react with the two first-row transition metal salts cobalt(II) and nickel(II) chlorides to boratrane complexes under activation of the boron hydrogen bond and reduction of the metal to give [M{B(Pn^R)$_3$}X] (M = Co, X = Cl; M = Co, X = η^2-Pn^R; M = Ni, X = Cl). Magnetic measurements and DFT studies support the experimentally determined spin states of the nickel(I) and cobalt(I) boratrane complexes. Furthermore, population analysis based on molecular orbitals indicates a polar metal−boron bond in both systems. The here reported ligands represent an important addition to the set of ligands allowing the formation of boratrane

Table 6. Crystallographic Data and Structure Refinement for Complexes $[K_2\{HB(Pn^{tBu})_2\}(H_2O)_3]$, **1**–**5**

	$[K_2\{HB(Pn^{tBu})_2\}(H_2O)_3]$	**1**	**2**	**3**	**4**	**5**
empirical formula	$C_{30}H_{38}B_2K_2N_{12}O_3S_6\cdot 3CH_3OH$	$C_{24}H_{33}BClN_6NiS_3\cdot CH_3OH$	$C_{15}H_{15}BClN_6NiS_3\cdot 0.5(Pn^{Me}S)_2\cdot CH_2Cl_2$	$C_{24}H_{33}BClCoN_6S_3\cdot 2CH_2Cl_2$	$C_{32}H_{44}BCoN_8S_4$	$C_{40}H_{28}BCoN_8S_4\cdot 3CHCl_3$
M_r, g/mol	992.95	638.76	690.58	776.79	738.73	1176.79
cryst description	plate, yellow	lozenge, red	block, red	needle, green	plate, black	block, black
cryst syst	trigonal	triclinic	monoclinic	monoclinic	monoclinic	triclinic
space group	$R\bar{3}$	$P\bar{1}$	$C2/c$	$P2_1/c$	$P2_1/c$	$P\bar{1}$
a, Å	13.7045(7)	9.421(2)	21.7054(6)	9.6463(5)	15.5146(5)	13.0774(5)
b, Å	13.7045(7)	12.321(2)	14.6737(4)	22.9979(12)	23.9519(8)	14.3589(5)
c, Å	45.762(4)	14.167(3)	20.0626(5)	16.2353(8)	9.9032(3)	14.3931(5)
α, deg	90	105.777(7)	90	90	90	99.276(2)
β, deg	90	99.126(9)	118.5540(10)	92.323(2)	105.3850(10)	111.6870(10)
γ, deg	120	95.234(7)	90	90	90	95.562(2)
vol, Å^3	7443.2(8)	1546.8(6)	5612.7(3)	3598.8(3)	3548.2(2)	2442.19(15)
Z	6	2	8	4	4	2
T, K	100(2)	100(2)	100(2)	100(2)	100(2)	100(2)
D_c, g/cm^3	1.329	1.371	1.634	1.434	1.383	1.600
μ(Mo Kα), mm^{-1}	0.495	0.945	1.304	1.050	0.755	1.058
F(000)	3084	670	2816	1600	1552	1188
reflns collected	17144	22785	75782	57339	48786	38021
unique reflns	3779	7690	9751	7036	9807	11136
reflns with $I \geq 2\sigma(I)$	2073	6099	7348	5812	8209	8748
R(int)	0.0525	0.0325	0.0502	0.0361	0.0310	0.0398
no. of params/restraints	168/0	354/0	347/0	402/0	427/4	560/0
final R1 [a], wR2 [b] ($I \geq 2\sigma$)	0.0736, 0.2273	0.0510, 0.1222	0.0402, 0.1101	0.0429, 0.0793	0.0316, 0.0736	0.0445, 0.1064
R indices (all data)	0.1161, 0.2402	0.0712, 0.1331	0.0580, 0.1157	0.0609, 0.0914	0.0430, 0.0804	0.0587, 0.1122
GOF on F^2	1.059	1.144	1.098	1.198	1.030	1.084
larg diff peak and hole, e/Å^3	1.032, −0.891	2.846, −0.692	0.848, −1.230	0.510, −0.492	0.782, −0.407	1.867, −1.067
data CCDC	785118	785380	785116	801057	785113	785114

[a] $R1 = \sum||F_o| - |F_c||/\sum|F_o|$. [b] $wR2 = \{\sum[w(F_o^2 - F_c^2)^2]^2/\sum[w(F_o^2)^2]\}^{1/2}$.

compounds. Their coordination chemistry we have only begun to explore. Due to the unique electronic properties as well as the additional donor site in the pyridazine heterocycle, these new scorpionates are expected to show a higher coordinative flexibility, which we are currently investigating.

Experimental Section

General. NMR spectra were measured on a Bruker Avance III 300 MHz spectrometer. ^{1}H NMR and ^{13}C NMR spectroscopy chemical shift values are reported as δ using the solvent signal (DMSO-d_6: δ 2.5 or 40 ppm, respectively) as an internal standard. Spectra were obtained at 25 °C. Mass spectra were measured on an Agilent LCMSD single quadrupole mass spectrometer of the SL type. The mass spectrometer was equipped with an atmospheric pressure ionization (API) source employing pneumatically assisted electrospray nebulization with nitrogen as the nebulizer gas. Elemental analyses were performed on a Heraeus VARIO ELEMENTAR by the Analytisch-Chemisches Laboratorium des Instituts für Anorganische Chemie der Technischen Universität Graz, Austria. Infrared spectra were recorded on a Perkin-Elmer FT-IR spectrometer 1725X as KBr pellets and on a Bruker Alpha Platinum ATR spectrometer.

Measurement of the magnetic susceptibility of the solid complexes was performed at ambient temperature on the modified Faraday balance SUS 10 (manufactured by A. Paar KG, Graz Austria). Typically, an amount of 10 to 20 mg of dry sample was placed in a small quartz tube. The signal was corrected for the diamagnetism of this tube. The balance was calibrated with Hg[Co(NCS)$_4$].[25] Routinely, the measurements were performed at four different magnetic fields (with flux densities: 0.42, 0.71, 1.02, and 1.32 T) to reveal the potential presence of any ferromagnetic impurities. The effective moment was obtained from the molar magnetic susceptibility χ_M via

$$\mu_{eff} = 797.5\sqrt{\chi_M T}\mu_B$$

where T is the temperature and μ_B the Bohr magneton, and the number n of unpaired electrons was calculated from the relation:

$$\mu_{eff} = \sqrt{n(n+2)}$$

Computational Details. All geometries were optimized in the gas phase using the BH-LYP,[22] B3-LYP[22b,c,23] and B-P[22a,24] DFT methods as implemented in the TURBOMOLE[26] program. Initial geometry optimizations as well as vibrational analysis were done with the standard double-ζ quality basis def2-SVP.[27]The geometries were reoptimized using the larger def2-TZVP basis.[27b,28] Input geometries were created from crystal structures. Mulliken Population Analysis (MPA), Natural Population Analysis (NPA)[29] and calculations of the Shared Electron Numbers (SEN)[30] were performed for the stationary points of the different spin states with the larger def2-TZVP basis. Visualizations of the molecule orbitals were performed using gOpenMol.[31]

X-ray Structure Determinations. For X-ray structure analyses for all compounds the crystals were mounted onto the tip of glass fibers and covered in inert oil. Data collection was performed on a BRUKER-AXS SMART APEX 2 CCD diffractometer using graphite-monochromated Mo Kα radiation (0.71073 Å) at 100(2) K. The data for all compounds were reduced to F_o^2 and corrected for Lp with SAINT.[32] Absorption

(25) Buenzli, J. C. G. *Inorg. Chim. Acta* **1979**, *36*, L413–L414.

(26) TURBOMOLE V6.2 2010, a development of University of Karlsruhe and Forschungszentrum Karlsruhe GmbH, 1989−2007, TURBOMOLE GmbH, since 2007; available from http://www.turbomole.com.

(27) (a) Schäfer, A.; Horn, H.; Ahlrichs, R. *J. Chem. Phys.* **1992**, *97*, 2571–2571. (b) Weigend, F.; Ahlrichs, R. *Phys. Chem. Chem. Phys.* **2005**, *7*, 3297–3305.

(28) Weigend, F.; Häsler, M.; Patzelt, H.; Ahlrichs, R. *Chem. Phys. Lett.* **1998**, *294*, 143–152.

(29) Reed, A. E.; Weinstock, R. B.; Weinhold, F. *J. Chem. Phys.* **1985**, *83*, 735–746.

(30) Ehrhardt, C.; Ahlrichs, R. *Theor. Chim. Acta* **1985**, *68*, 231–245.

(31) (a) Laaksonen, L. *J. Mol. Graphics* **1992**, *10*, 33–34. (b) Bergman, D. L.; Laaksonen, L.; Laaksonen, A. *J. Mol. Graphics Modell.* **1997**, *15*, 301–306.

correction was performed with SADABS.[33] The structures were solved by direct methods[34] using the WinGX suite of programs[35] and refined by the full-matrix least-squares method with SHELXS-97.[36] If not noted otherwise all non-hydrogen atoms were refined with anisotropic displacement parameters. All hydrogen atoms were fixed in calculated positions to correspond to standard bond lengths and angles. In the case of complexes **1** and **5**, as well as the $K[HB(Pn^{Me})_3]$, disordered solvent molecules are present in the structures and their contributions were removed from the data set with the help of the PLATON SQUEEZE routine.[37]

Syntheses of Pyridazinethiones. The starting materials 6-methylpyridazin-3-one and 6-*tert*-butylpyridazin-3-one were synthesized according to literature methods.[38,39]

6-*tert*-Butylpyridazine-3-thione (HPn^{tBu}). A mixture of 6-*tert*-butylpyridazin-3-one (100 g, 0.657 mol) and phosphorpentasulfide (146 g, 0.657 mol) was stirred under reflux in pyridine (1 L) for 2 h. After cooling to room temperature, the dark brown solution was poured on stirred ice−water (2 L), resulting in precipitation of yellow crystals, which were isolated by filtration and washed with cold water (300 mL). The crystals were dissolved in ethanol (800 mL), and the solution was heated and treated with charcoal. While still hot the mixture was filtered and allowed to cool to room temperature. The yellow precipitate was collected and dried giving 87 g (61%) of the thione. ^{1}H NMR (DMSO-d_6, 300 MHz): δ 1.20 (s, 9H, *tert*-butyl-CH_3), 7.46 (d, 1H, $^3J_{H-H}$ = 9.4 Hz, *H*5), 7.55 (dd, $^3J_{H-H}$ = 9.4 Hz, $^4J_{N-H}$ = 2.1 Hz, *H*4), 14.50 (s, 1H, N*H*) ppm. ^{13}C NMR (DMSO-d_6, 75 MHz): δ 28.4 (*tert*-butyl-*C*H_3), 35.9 (*t*-Bu-*C*), 125.4 (C5), 140.7 (C4), 160.2 (C6), 178.1 (C=S) ppm. MS (ESI): m/z = 168 ($[M]^+$) 100%. IR (KBr pellets, cm^{-1}): 1790 s, 1565 s, 1402 s, 1146 s, 839 s, 641 m.

6-Methylpyridazine-3-thione (HPn^{Me}). The compound was synthesized according to the procedure described in the literature, however NMR spectroscopy data were not reported.[15] ^{1}H NMR (DMSO-d_6, 300 MHz): δ 2.29 (s, 3H, CH_3), 7.18 (d, 1H, $^3J_{H-H}$ = 9.1 Hz, *H*5), 7.52 (dd, $^3J_{H-H}$ = 9.1 Hz, $^4J_{N-H}$ = 2.0 Hz, *H*4), 14.49 (s, 1H, N*H*) ppm. ^{13}C NMR (DMSO-d_6, 75 MHz): δ 20.2 (*C*H_3), 128.6 (*C*5), 140.3, (*C*4), 150.7 (*C*6), 178.0 (C=S) ppm.

Syntheses of Scorpionate Ligands. Potassium Hydrotris(6-*tert*-butylpyridazine-3-thionyl)borate ($K[HB(Pn^{tBu})_3]$). Under an argon atmosphere, potassium borohydride (0.64 g, 12 mmol) and 6-*tert*-butylpyridazine-3-thione (6.00 g, 36 mmol) were suspended in diphenylmethane (8 mL). The suspension was gradually heated to 190 °C over a period of 2 h. After an additional hour of stirring, evolution of H_2 gas ceased and the reaction mixture was allowed to cool to room temperature. The resulting precipitate was isolated by filtration, washed with hot cyclohexane (75 mL) and dried in vacuo to give 3.95 g (60%) of the ligand as a yellow powder. Recrystallization from methanol gave single crystals suitable for X-ray diffraction analyses which confirmed the formation of the salt. ^{1}H NMR (DMSO-d_6, 300 MHz): δ 0.91 (s, 9H, CH_3), 7.02 (d, 1H, $^3J_{H-H}$ = 9.1 Hz, *H*5), 7.39 (d, 1H, $^3J_{H-H}$ = 9.1 Hz, *H*4) ppm. ^{13}C NMR (DMSO-d_6, 75 MHz): δ 28.5 (*t*-Bu *C*H_3), 35.7 (*t*-Bu-*C*), 120.0 (C5), 141.3 (C4), 156.1 (C6), 180.2 (C=S) ppm. MS (ESI) m/z = 513 ($[M - K]^-$) 100%. IR (KBr pellets, cm^{-1}): 2963 m, 1478 m, 1428 s, 1240 m, 1210 s, 1144 m, 1004 m. Anal. Calcd for $C_{24}H_{34}N_6BKS_3$: C, 52.16; H, 6.20; N, 15.21%. Found: C, 52.27; H, 6.39; N, 15.32%.

Potassium Hydrotris(6-methylpyridazine-3-thionyl)borate ($K[HB(Pn^{Me})_3]$). Under an argon atmosphere, potassium borohydride (0.85 g, 16 mmol) and 6-methylpyridazine-3-thione (6.00 g, 48 mmol) were suspended in diphenylmethane (13 mL). The suspension was gradually heated to 169 °C over a period of 2 h after which H_2 evolution ceased. The suspension was allowed to cool to 120 °C. The precipitate was filtered and washed with hot cyclohexane (170 mL) and methanol (30 mL). Drying in vacuo gave 2.84 g (42%) of the ligand as a yellow powder. Crystals suitable for X-ray diffraction analysis were obtained by recrystallization from methanol. ^{1}H NMR (DMSO-d_6, 300 MHz): δ 2.05 (s, 3H, CH_3), 6.80 (d, 1H, $^3J_{H-H}$ = 9.00 Hz, *H*5), 7.34 (d, 1H, $^3J_{H-H}$ = 9.00 Hz, *H*4) ppm. ^{13}C NMR (DMSO-d_6, 75 MHz): δ 21.10 (*C*H_3), 123.51 (C5), 141.26 (C4), 146.74 (C6), 180.35 (C=S) ppm. MS (ESI): m/z = 387 ($[M - K]^-$) 100%. IR (KBr pellets, cm^{-1}): 1610 w, 1510 w, 1428 s, 1222 s, 1111 s, 999 m, 615 m. Anal. Calcd for $C_{15}H_{16}N_6BKS_3 \cdot 0.95H_2O$: C, 40.97; H, 4.10; N, 19.12%. Found: C, 40.97; H, 3.80; N, 19.00%.

Syntheses of the Complexes. $[Ni\{B(Pn^{tBu})_3\}Cl]$ (1). A stirred solution of $K[HB(Pn^{tBu})_3]$ (0.30 g, 0.54 mmol) in CH_2Cl_2 (35 mL) was treated with $NiCl_2$ (0.070 g, 0.54 mmol). After 10 h of stirring, the dark brown reaction mixture was filtered and the solvent was removed in vacuo. Recrystallization from a methanol solution gave dark red crystals. They were isolated by filtration and washed with tetrahydrofuran, giving 0.062 mg (19%) of **1**. Crystals suitable for X-ray diffraction analysis were obtained by recrystallization from a methanol solution. Mp: 230 °C (dec). MS (ESI): m/z 570 (68%) $[M - Cl]^+$. IR (KBr pellets, cm^{-1}) 1593 w, 1477 m, 1434 s, 1144 m, 916 w, 649 w. Anal. Calcd for $C_{24}H_{33}N_6BClNiS_3$: C, 47.51; H, 5.48; N, 13.85%. Found: C, 47.52; H, 4.43; N, 13.78%.

Alternative Synthesis of $[Ni\{B(Pn^{tBu})_3\}Cl$ (1). A stirred solution of $K[HB(Pn^{tBu})_3]$ (0.20 g, 0.36 mmol) in H_2O (25 mL) was treated with $NiCl_2 \cdot 6H_2O$ (0.086 g, 0.36 mmol), resulting in immediate formation of a dark red precipitate. The suspension was stirred for 15 min, and the product was isolated by filtration and dried in vacuo overnight. Recrystallization from dichloromethane/diethyl ether solution (1:1 v/v) gave dark red crystals. They were isolated by filtration and washed with tetrahydrofuran giving 0.054 g (25%) of **1**.

$[Ni\{B(Pn^{Me})_3\}Cl]$ (2). A stirred solution of $K[HB(Pn^{Me})_3]$ (0.96 g, 2.3 mmol) in H_2O (120 mL) was treated with $NiCl_2 \cdot 6H_2O$ (0.535, 2.3 mmol), resulting in immediate formation of a dark red precipitate. The suspension was extracted with 100 mL of CH_2Cl_2 and dried with Na_2SO_4. After evaporation of the solvent, a dark red powder was obtained. Recrystallization from dichloromethane/diethyl ether solution (1:1 v/v) gave dark red crystals. They were isolated by filtration and washed with tetrahydrofuran, giving 0.37 g (34%) of **2**. Crystals suitable for X-ray diffraction analysis were obtained from the precipitated material prior to washing with THF by recrystallization from a dichloromethane/diethyl ether solution (1:1 v/v) revealing one molecule of **2** and $(SPhMe)_2$ in the unit cell. Mp: 230 °C (dec). MS (ESI): m/z 444 (100%) $[M - Cl]^+$. IR (KBr, cm^{-1}): 1541 w, 1418 s, 1040 m, 829 m. Anal. Calcd for $C_{15}H_{15}N_6BClNiS_3$: C, 37.50; H, 3.15; N, 17.49%. Found: C, 37.49; H, 1.57; N, 17.39%.

$[Co\{B(Pn^{tBu})_3\}Cl]$ (3). To a stirred solution of $K[HB(Pn^{tBu})_3]$ (0.30 g, 0.54 mmol) in CH_2Cl_2 (35 mL) was added $CoCl_2$ (0.071 g, 0.54 mmol). After 10 h of stirring, the dark green reaction mixture was filtered and the solvent was removed in vacuo. Recrystallization from a dichloromethane solution gave dark green crystals. They were isolated by filtration and washed with tetrahydrofuran, giving 150 mg (46%) of **3**. Crystals suitable for X-ray diffraction analysis were obtained by recrystallization

(32) *SAINTPLUS: Software Reference Manual*, version 6.4; Bruker AXS: Madison, WI, 1997.
(33) (a) Blessing, R. H. *Acta Crystallogr. Sect. A: Found. Crystallogr.* **1995**, *A51*, 33–38. (b) *SADABS*, version 2.1; Bruker-AXS: Madison, WI, 1998.
(34) Sheldrick, G. M. *SHELXS-97*; University of Göttingen: Göttingen, Germany, 1997.
(35) Farrugia, L. J. *J. Appl. Crystallogr.* **1999**, *32*, 837–838.
(36) Sheldrick, G. M. *Acta Crystallogr., Sect. A: Found. Crystallogr.* **2008**, *64*, 112–122.
(37) Spek, A. L. *J. Appl. Crystallogr.* **2003**, *36*, 7–13.
(38) Overend, W. G.; Wiggins, L. F. *J. Chem. Soc.* **1947**, 239–244.
(39) Coates, W. J.; McKillop, A. *Synthesis* **1993**, 334–342.

from a dichloromethane solution. Mp: 255 °C (dec). MS (ESI): m/z 571 (100%) $[M - Cl]^+$. IR (ATR, cm^{-1}): 2963 m, 1588 m, 1476 s, 1426 s, 1209 s, 1174 s, 920 s, 849 m, 649 s. Anal. Calcd for $C_{24}H_{33}BClCoN_6S_3$: C, 47.49; H, 5.48; N, 13.85%. Found: C, 47.48; H, 5.51; N, 13.92%.

[Co{B(Pn^{tBu})$_3$}(Pn^{tBu})] (4). To a stirred solution of K[HB(Pn^{tBu})$_3$] (0.20 g, 0.36 mmol) in H_2O (25 mL) was added $CoCl_2 \cdot 6H_2O$ (0.0857 g, 0.36 mmol). The formation of a dark green precipitate was immediately apparent. The suspension was stirred for 15 min at room temperature, and the green powder was isolated by filtration and dried in vacuo overnight. Recrystallization from dichloromethane/diethyl ether solution (1:1 v/v) gave green crystals. They were isolated by filtration and washed with tetrahydrofuran, giving 0.053 g (20%) of **4**. Crystals suitable for X-ray diffraction analysis were obtained by recrystallization from a dichloromethane/diethyl ether solution (1:1 v/v). Mp: 225 °C (dec). MS (ESI): m/z 739 ($[M + H]^+$) 5%, 571 ($[M - Pn^{tBu}]^+$) 100%. IR (KBr pellets, cm^{-1}): 2963.5 s, 1589 w, 1477 s, 1435 s, 1210 s, 1142 s, 914 w, 835 m.

Supporting Information Available: CIF file. This material is available free of charge via the Internet at http://pubs.acs.org.